A Tail Fiber Protein and a Receptor-Binding Protein Mediate ICP2 Bacteriophage Interactions with *Vibrio cholerae* OmpU

Andrea N.W. Lim[a], Minmin Yen*, Kimberley D. Seed*, David W. Lazinski, Andrew Camilli[#]

Department of Molecular Biology and Microbiology, Tufts University, School of Medicine, Boston, Massachusetts, USA

[a]Department of Molecular Biology and Microbiology, Graduate School of Biomedical Sciences, Tufts University, School of Medicine, Boston, Massachusetts, USA

Running title: Identification of two ICP2 tail fiber proteins

#Address correspondence to Andrew Camilli, andrew.camilli@tufts.edu.

*Present address: Minmin Yen, PhagePro, Inc., Boston, Massachusetts, USA.

*Present address: Kimberley D. Seed, Department of Plant and Microbial Biology, University of California, Berkeley, Berkeley, California, USA.

Abstract

ICP2 is a virulent bacteriophage (phage) that preys on *Vibrio cholerae*. ICP2 was first isolated from cholera patient stool samples. Some of these stools also contained ICP2-resistant isogenic *V. cholerae* strains harboring missense mutations in the trimeric outer membrane porin protein OmpU, identifying it as the ICP2 receptor. In this study, we identify the ICP2 proteins that mediate interactions with OmpU by selecting for ICP2 host-range mutants within infant rabbits infected with a mixture of wild type and OmpU mutant strains. ICP2 host-range mutants had missense mutations in putative tail fiber gene *gp25* and putative adhesin *gp23*. Using site-specific mutagenesis we show that single or double mutations in *gp25* are sufficient to generate the host-range mutant phenotype. However, at least one additional mutation in *gp23* is required for robust plaque formation on specific OmpU mutants. Mutations in *gp23* alone were insufficient to give a host-range mutant phenotype. All ICP2 host-range mutants retained the ability to plaque on wild type *V. cholerae* cells. The strength of binding of host-range mutants to *V. cholerae* correlated with plaque morphology, indicating that the selected mutations in *gp25* and *gp23* restore molecular interactions with the receptor. We propose that ICP2 host-range mutants evolve by a two-step process where, first, *gp25* mutations are selected for their broad host-range, albeit accompanied by low level phage adsorption. Subsequent selection occurs for *gp23* mutations that further increase productive binding to specific OmpU alleles, allowing for near wild type efficiencies of adsorption and subsequent phage multiplication.

Importance

Concern over multidrug-resistant bacterial pathogens, including *Vibrio cholerae*, has led to a renewed interest in phage biology and their potential for phage therapy. ICP2 is a genetically unique virulent phage isolated from cholera patient stool samples. It is also one of three phages

in a prophylactic cocktail shown to be effective in animal models of infection and the only one of the three that requires a protein receptor (OmpU). This study identifies a ICP2 tail fiber and a receptor binding protein and examines how ICP2 responds to the selective pressures of phage-resistant OmpU mutants. We found that this particular co-evolutionary arms race presents fitness costs to both ICP2 and *V. cholerae.*

Introduction

Vibriophages, phages that prey on bacteria from the gram-negative *Vibrio* genus, were first described by E.H. Hankin in 1896 as antimicrobial agents from the Ganges River, two decades before phages were formally identified by Twort and d'Herelle (1, 2). Growing concern over the emergence of multidrug-resistant strains of *Vibrio cholerae* (3), the causative agent of cholera, has renewed scientific interest in vibriophages as therapeutics (2, 4) and environmental markers of cholera outbreaks (5-7). In 2011, our lab isolated three unique virulent vibriophages from the rice-water stools of Bangladeshi cholera patients, designated phages ICP1, ICP2, and ICP3 (7). ICP2 is morphologically categorized as a short-tailed podovirus but bears little genetic homology to the canonical podovirus T7 or other members of the family. Its 50 kb genome encodes 73 putative protein coding sequences divided into two transcriptional units in opposite orientations.

An isolate of ICP2 was also recovered in 2014 from the rice-water stool of a Haitian cholera patient (8). This sample also contained several ICP2-resistant isogenic *V. cholerae* strains that had missense mutations in *ompU*. OmpU is an outer membrane general porin that is associated with virulence (9-11), adherence (12), and osmoregulation (13-15). ICP2-resistant strains with null mutations in *toxR* were also found among several stool samples containing

ICP2. ToxR is a transcriptional activator of virulence genes including *ompU*. Accordingly, the *toxR* null mutations resulted in attenuated *V. cholerae* colonization in an infant mouse model as well as the complete loss of *ompU* expression (9). Further experiments showed that two OmpU missense mutations, V324F and G325D, only minimally affect *V. cholerae* fitness. These mutations identified OmpU as the ICP2 receptor and demonstrated how vibriophages impose selective pressures during cholera infections.

In 2018, two groups solved the crystal structure of *V. cholerae* OmpU (16, 17). OmpU is an outer membrane localized homotrimer, with each monomer comprised of a 16-β-stranded barrel. Each monomer has a central pore of ~0.55-0.6 nm wide (17) and has 8 protruding extracellular loops (Figure 1). L2 projects into the neighboring monomer, while L3 is a constriction loop that bends into the center of each barrel. The OmpU residues that mutated to confer ICP2 resistance in the stool samples (8) are highlighted on one monomer-monomer interface in Figure 1 (8, 16). All mutations, except N158Y, are in L4 and L8. These extracellular loops are adjacent between neighboring monomers. N158Y is found near the transmembrane region of L3, and its affect on OmpU localization or structure are unknown. These observations suggest that ICP2 binds *V. cholerae* at the L4 and L8 interfaces of OmpU trimers. We sought to identify the ICP2 proteins that interact with OmpU and examine how ICP2 may counter-evolve in response to phage-resistant *V. cholerae* OmpU mutants.

Results

ICP2 host-range mutants have missense mutations in *gp23* and *gp25*

ICP2 host-range mutants were selected during intestinal infection of infant rabbits co-inoculated with ICP2 and a mixture of *V. cholerae* wild type (WT) and OmpU point mutant strains at a 10:1 ratio. The addition of WT *V. cholerae* was designed to allow for enough replication of ICP2 to yield spontaneous host-range mutants that could then be enriched by replicating on the OmpU mutants. Until the appearance of such host-range mutants, the OmpU mutants have a competitive advantage over WT *V. cholerae* due to lack of predation by ICP2. Indeed, this was shown previously when ICP2 predation resulted in a 10,000-fold competitive advantage for OmpU G325D over the WT after 12 hours of infection of infant rabbits (8). One group of four animals was inoculated with WT *V. cholerae* and a mixture of OmpU A196_Y198dup, OmpU A195T, OmpU L319R, and OmpU S329L. A second group of four animals was inoculated with WT and a mixture of OmpU A182_T193dup, OmpU V324F, and OmpU N158Y. A third group of four animals was infected with WT and OmpU G325D. ICP2 in cecal fluid obtained from euthanized symptomatic animals was plaqued on soft agarose overlays containing specific OmpU mutants to isolate host-range mutants. These included OmpU mutants A195T, V324F, and G325D. Up to seven plaques per host strain per animal were chosen for plaque purification on each respective OmpU mutant. All plaques were clear and of equivalent size as those formed by WT ICP2 on WT *V. cholerae*.

The ICP2 host-range mutants were whole-genome sequenced to identify possible mutations. Of the 28 isolates sequenced, thirteen were unique (Figure 2A). Those isolated on OmpU V324F or OmpU G325D contained multiple single nucleotide variants (SNVs) in *gp23* and *gp25* (Figure 2), each a missense mutation. This strongly implicates Gp23 and/or Gp25 as

ICP2 proteins that interact with the OmpU receptor. According to homology analysis via Interative Threading Assembly Refinement (I-TASSER) (18-20) and the Rapid Annotation using Subsystem Technology version 2 (RAST) (21, 22), *gp23* encodes a putative receptor binding adhesin protein and *gp25* encodes a putative phage tail fiber. Although *gp24* is also annotated as a putative tail fiber, no mutations were found in this gene. It is unlikely that Gp23 and Gp25 are tail tube proteins because those have previously been identified bioinformatically as Gp9, Gp10, and Gp11 (23).

ICP2 mutants isolated on OmpU V324F have a Gp23 S188A mutation, while those isolated on OmpU G325D have a Gp23 S209R mutation (Figure 2). Gp25 mutations were more prevalent and varied among the ICP2 host-range mutants. Gp25 mutations clustered near the N- and C-termini, which are outside or near the ends of two predicted collagen fiber-like domains (Figure 2). Gp25 mutations exhibit loose specificity for individual OmpU alleles. Residues Q510 and N690 both mutated to different amino acids in different ICP2 phages isolated on the OmpU G325D mutant. In contrast, a single S742P mutation was shared among phages isolated on both OmpU V324F and G325D mutants. Because these ICP2 host-range mutants were selected during intestinal infection, we could not determine how many rounds of phage replication occured before developing the ability to infect an OmpU mutant nor the order in which Gp23 and Gp25 mutations were selected. Therefore, we next sought to parse the relationship between the ICP2 Gp23 and Gp25 mutations and *V. cholerae* OmpU alleles.

ICP2 host-range mutants require at least one Gp25 mutation

Plasmid-based recombination in *V. cholerae* was used to generate ICP2 mutants with the *gp25* mutations identified in VF(2), GD(6), and GD(1). Host-range mutants are herein named for the OmpU mutant host on which they were isolated followed by a unique identifying number.

VF(2) and GD(6) both contain a Gp25 S742P mutation despite being isolated on different OmpU mutants. Gp25 in GD(6) also contains a unique second K159E mutation. GD(1) contains Gp25 D96N and S676A mutations. Recombinant plaques with single Gp25 S742P mutations, derived from VF(2) or GD(6), were isolated and plaque-purified once on OmpU V324F and then amplified on WT. GD(1) recombinants were isolated and plaque-purified once on OmpU G325D and then amplified on WT. We chose to amplify on WT instead of an OmpU mutant in order to limit further selection for spontaneous mutations that might increase infectivity on the latter host. All host-range mutants isolated in this study formed clear, normal sized plaques on WT, suggesting there would not be selective pressure for additional mutations on this host. Control recombination infections using a plasmid containing WT *gp23* and *gp25* did not result in any host-range mutants. The recombinant mutants were whole-genome sequenced to verify mutations. Recombinant mutants are designated with an "R" and a unique identifying number following their parent name (Figure 2C).

Efficiency-of-plaquing (EOP) assays were used to quantify how efficiently these mutants can infect OmpU V324F and G325D relative to WT cells. Low EOPs often correlated with a turbid plaque morphology (Figure 3A). Recombinant ICP2 mutants with only one or two Gp25 mutations maintain the ability to form clear plaques on WT host cells but can only weakly form plaques, i.e., low EOPs and turbid plaques, on either OmpU V324F or OmpU G325D. No host-range mutants formed plaques on a Δ*ompU* control, indicating that they are interacting with either OmpU V324F or G325D and not another receptor. Isolates VF(2)R1 and GD(6)R1 are biological duplicates with a Gp25 S742P mutation. While they form turbid plaques on both OmpU V324F and G325D, their EOP on OmpU V324F is only 10-fold lower than on WT (Figure 3A). In contrast, their EOPs on OmpU G325D are 4- to 5-logs lower than on WT.

GD(1)R1 and GD(1)R2, with Gp25 mutations D96N and S676A, also form turbid plaques on both OmpU V324F and G325D. These phage mutants have a clear preference for OmpU G325D, with GD(1)R2 barely reaching a statistically significant EOP on OmpU V324F. While Gp25 mutations alone do not provide robust phenotypes, at least one is required to weakly infect an OmpU mutant.

Further support for the important role of Gp25 in conferring a host-range phenotype came from host-range mutants evolved in animals and then isolated on OmpU A195T, a host strain only partially resistant to WT ICP2 (8). These phage mutants have one or two mutations in Gp25 and no mutations in Gp23 (Figure 2A). This provides further evidence that Gp25 mutations are sufficient to expand host-range.

In host-range assays that included five additional ICP2-resistant OmpU mutants, ICP2 mutants with only one or two Gp25 mutations and no Gp23 mutations exhibit a similar host-range pattern despite the diversity of their Gp25 mutations (Figure 4, top eight ICP2 mutants). In addition to forming clear plaques on WT *V. cholerae*, most of these host-range mutants have higher EOPs on OmpU L319R, S329L, and A182_T193dup. This suggests that initial Gp25 mutations are necessary and sufficient to expand host-range.

Selection of ICP2 host-range mutants *in vitro*

The observation that all ICP2 host-range mutants isolated in animals retain the ability to plaque on WT *V. cholerae* could be due to fact that both WT and OmpU mutants were present during the selection. To investigate this hypothesis, we sought to isolate host-range mutants *in vitro* on pure cultures of the OmpU A182_T193dup strain and then test plaque formation on WT *V. cholerae*. Initial attempts to select ICP2 host-range mutants *in vitro* failed, likely due to lack of a sufficiently large enough pool of input phage to harbor preexisting mutants. To overcome

this limitation, we generated two independent high-titer stocks of ICP2 on a mutator strain of *V. cholerae* in which the mismatch repair gene *mutS* was deleted. Deletion of *mutS* was previously shown to increase the mutation rate of *V. cholerae* by 100-fold (24). Although it is not known if the host methyl-directed mismatch repair system functions with ICP1 DNA replication, it is notable that ICP1 encodes its own DNA adenine methyltransferase (Dam) (8). After two rounds of selection on the OmpU A182_T193dup strain, host-range mutants that form clear plaques were obtained. Whole-genome sequencing of four ICP2 host-range mutants from each independent selection yielded a total of four lineages; one from the first and three from the second selection. Previously observed and novel mutations in *gp25* were found, but no mutations in *gp23* were present (Figure 2B). Two mutants contained the previously observed single Gp25 S742P mutation. Only the three host-range mutants with novel Gp25 mutations are shown in Figure 2B and were further analyzed. These results are consistent with those obtained from the *in vivo* selected host-range mutants, in that mutations in Gp25 are sufficient to give a host-range phenotype on an OmpU A182_T193dup strain.

Next, we compared EOP and plaque phenotype on OmpU A182_T193dup and WT *V. cholerae.* The three host-range mutants formed clear plaques on OmpU A182_T193dup and, as observed for the *in vivo* selected host-range mutants, all retained clear plaque formation on WT *V. cholerae* (Figure 4, rows 9-11). Consistent with this, their EOPs on OmpU A182_T193dup and WT were at or near 1. These mutants formed turbid plaques on OmpU L319R and S329L, similar to the other Gp25-only mutants. Therefore, retention of infection of WT *V. cholerae* in ICP2 host-range mutants appears to be a general phenomenon, and not the result of selection in the presence of WT and an OmpU mutant.

Secondary Gp23 mutations increase EOP on specific OmpU mutants

To attempt to isolate ICP2 host-range mutants with only Gp23 mutations, WT *V. cholerae* with plasmids containing *gp23* S188A or S209R alleles were infected with WT ICP2. However, no recombinant plaques could be isolated on OmpU V324F or G325D. When the population of progeny phages from these infections were sequenced ~1% of the phage were found to have the intended mutations. Therefore, it appears that Gp23 mutations alone are insufficient to give a host-range phenotype.

A secondary Gp23 S188A in Gp25-only mutants imparts clear plaque formation on OmpU V324F. Host-range mutants with secondary Gp23 mutations were generated by using the ICP2 recombinants with one or two Gp25 mutations to infect WT cells containing plasmids containing either *gp23* S188A or S209R alleles. The addition of a Gp23 S188A leads to more efficient plaquing on OmpU V324F for all seven recombinants regardless of initial Gp25 mutations (Figure 3B). VF(2), VF(2)R2, and GD(6)R2 are biological triplicates containing Gp25 S742P and S188A, but were generated in an animal and *in vitro*, respectively. GD(1)R3, GD(1)R4, GD(1)R5, GD(1)R6, and GD(1)R7 contain Gp25 D96N and S676A from GD(1), as well as one to two novel Gp25 mutations (Figure 2C). Gp23 S188A was not seen with these combinations of Gp25 mutations among the host-range mutants evolved *in vivo*.

Similarly, a secondary Gp23 S209R mutation results in increased EOPs and/or clear plaque formation for all five recombinants on OmpU G325D regardless of initial Gp25 mutations (Figure 3C). VF(2)R3, containing Gp25 S742P and Gp23 S209R, was the only recombinant that still forms turbid plaques on OmpU G325D, but its EOP of 0.19 is markedly higher than that of Gp25 S742P mutant VF(2)R1, which has a mean EOP of 2.3×10^{-5}. The additional Gp25 K159E mutation in GD(6) increased the EOP further and gave clear plaques on OmpU G325D. The presence of Gp25 S742P also likely allows both GD(6) and VF(2)R3 to

form turbid plaques on OmpU V324F. GD(1)R9 and GD(1)R10 both have novel Gp25 mutations in addition to S676A and D96N mutations present in GD(1), while GD(1)R11 has a second Gp23 N190K mutation. These new mutations, however, do not result in EOPs on OmpU V324F and G325D that greatly differ from GD(1) or GD(1)R8 (Figure 3C). These results suggest that Gp23 mutations increase infection in a mostly allele-specific manner with respect to OmpU mutants, while retaining wild-type infection of WT OmpU.

In EOP assays that included five additional OmpU mutants, ICP2 mutants with secondary Gp23 mutations have modest alterations in host range (Figure 4). The middle 9 rows in Figure 4 show the host range of mutants with secondary Gp23 S188A mutations and the mutants in the final 12 rows all have a secondary Gp23 S209R mutation. The addition of a secondary Gp23 S188A mutation in VF(2), VF(2)R2, and GD(6)R2 corresponds with an inability to form plaques on OmpU L319R and S329L. VF(2)R2 and GD(6)R2 were derived from VF(2)R1 and GD(6)R1, which contain a single Gp25 S742P mutation and could previously infect these strains. VF(2)R3 contains the same single Gp25 S742P mutation and a secondary Gp23 S209R mutation but retains the ability to infect OmpU S329L and very weak infection of OmpU V324F. In addition to secondary Gp23 mutations, the presence of novel Gp25 missense mutations may also be playing a role in the host ranges of the remaining ICP2 mutants.

ICP2 host-range mutants can bind to OmpU mutants

If plaque formation on OmpU V324F and G325D requires direct binding by Gp23 and/or Gp25, binding to these OmpU alleles should correlate with EOP. We assayed binding over a period of 24 hours (hrs) to heat-killed host cells and quantified binding as the ratio of remaining free phage titer to the initial titer at t = 0 hrs. Cells were heat-killed by incubating at 51°C for 12 minutes (min) in a PCR thermocycler. The structure of the cells was unaffected by this treatment

as determined by phase-contract microscopy. WT ICP2 bound to WT *V. cholerae* between 10- and 100-fold, depending on the experiment, but did not exhibit any OmpU-independent binding to the *ΔompU* strain. ICP2 host-range mutants all retain the ability to significantly bind WT *V. cholerae* (Figure 5).

VF(2)R1 and GD(1)R1 show no binding to OmpU V324F and G325D (Figure 5), respectively. Because these phage mutants could form turbid plaques and had low to intermediate EOPs on these hosts, this suggests that the binding assay is not as sensitive. ICP2 mutants with a Gp23 S188A mutation, GD(6)R2 (Figure 5A), GD(1)R3, and GD(1)R7 (Figure 5B), all bind to OmpU V324F, as expected considering these phage mutants have high EOPs and form clear plaques. Similarly, VF(2)R3 (Figure 5A), GD(1)R8, GD(1)R9, and GD(1)R11 (Figure 5B) contain Gp23 S209R and bind to OmpU G325D. The one exception to this trend is that GD(1)R7, despite not forming plaques or having a detectable EOP on OmpU G325D, binds to both OmpU alleles with a preference for OmpU V324F.

In general the host-range mutants bind better to WT cells than to OmpU V324F and G325D mutants. VF(2)R1 has no detectable binding to either OmpU V324F or G325D. GD(6)R2 and VF(2)R3 show 99% binding to WT *V. cholerae*, but 95% and 91% binding to OmpU V324F and G325D, respectively (Figure 5A). Host-range mutants with significant binding to OmpU V324F or G325D are derived from GD(1)R1 or GD(1)R2 and have an additional Gp25 mutation (Figures 2B, 5B). The additional Gp23 mutation in GD(1)R11 does not significantly aide binding to OmpU G325D.

ICP2 host-range mutants prey on OmpU mutants in broth culture with varying efficiencies

The binding assays demonstrated that phage predation in broth culture differs from the slower diffusion of soft agar overlays in that the on-off rate of receptor binding will have a larger

impact on the rate of adsorption. Therefore, we conducted predation assays in shaking broth cultures to examine how the ICP2 phenotypes seen in EOP and binding assays are reflected on host cell killing. The cell density of early exponential growth phase *V. cholerae* cultures infected with ICP2 host-range mutants (MOI ~1) was measured as the optical density at 600 nm over 16 hrs at 37°C. As previously reported (8), the negative control *ΔompU* strain has a slight growth defect in LB (Figure 6A). All ICP2 host-range mutants prey on WT cells, suppressing exponential growth for ~6 hrs, followed by a return to exponential growth (Figure 6). Most *V. cholerae* cells replicating after 6 hrs have gained phage resistance (Table S1).

In contrast, VF(2)R1, GD(1)R1, and GD(1)R2 do not affect the growth of OmpU V324F or OmpU G325D (Figure 6A), correlating with their lack of binding as shown in Figure 5. These host-range mutants did, however, form turbid plaques and had measurable EOPs on these hosts, presumably due to the slower diffusion of host cells in plaque assays that allows even weak binding phages to eventually infect cells.

ICP2 recombinants with secondary Gp23 mutations specifically prey on either OmpU V324F or OmpU G325D, but not both. Correlating with the intermediate levels of binding in Figure 5, secondary Gp23 mutations result in moderate effects on OmpU V324F or OmpU G325D replication (Figure 6B and C). No host-range mutants tested were able to kill both OmpU V324F and G325D. VF(2)R2 (biological replicate of GD(6)R2) and VF(2)) blocks OmpU V324F late exponential phase. GD(1)R3 and GD(1)R7 do not disrupt OmpU G325D growth consistent with their low EOP (Figure 3B) and weak binding (Figure 5B) on this host.

GD(1)R8, GD(1)R9, GD(1)R10, and GD(1)R11 similarly block OmpU G325D late exponential phase. GD(1)R9 and GD(1)R10 infections lead to a much greater delay than GD(1)R8, despite all three phages having significant EOPs on OmpU G325D (Figure 3C, 6C).

Both GD(1)R9 and GD(1)R8 also bind OmpU G325D (Figure 5B). VF(2)R3 has no impact on OmpU G325D growth, correlating with its turbid plaque morphology and reduced EOP (Figure 5C). This further reinforces the necessity of the second Gp25 K159E mutation in GD(6).

Discussion

A model of ICP2 evolution within humans

During *V. cholerae* infection in people, the presence of ICP2 phage in the intestinal tract imposes selective pressure, resulting in the appearance of phage escape mutants with mutations in the OmpU receptor. In this scenario, we hypothesize that ICP2 *gp25* mutations are initially selected for increased generalized binding to several OmpU mutants. This generalized binding allows for minimal infection of some OmpU mutant hosts, expanding these phage mutants in the population. Further selection for secondary *gp23* mutations allows for more efficient infection of specific OmpU alleles but comes with the risk of a limited host-range. For example, phages with Gp23 S188A mutations have a narrow host-range and only five of the nine mutants gained an appreciable ability to plaque on one to two additional OmpU alleles. Phages with Gp23 S209R mutations have a wider host-range, with ten of 12 mutants gaining the ability to plaque on three or four additional OmpU alleles.

V. cholerae forces ICP2 to generate a variety of different *gp25* and *gp23* mutations, while tempering fitness costs to itself by maintaining a population of functional OmpU alleles (8). This model parallels the one described by DeSordi et al. (25) in which phages infect “intermediate” hosts in the microbiome while evolving towards an expanded host-range. Initial ICP2 host-range mutants with *gp25* mutations are in the process of “jumping” between different OmpU alleles as

316 intermediate hosts. Further studies need to be done to determine if this selective process involves
317 infection processes downstream of OmpU binding, such as DNA injection or virion assembly.

318 **A model of ICP2 tail fiber structure**

319 Speculation into ICP2 tail fiber structure can be made based on the step-wise evolution of
320 Gp25 and Gp23 and current literature on phage tail fibers and receptor binding proteins (RBPs).
321 Although morphologically in the *Podoviridae* family (7), ICP2 Gp23, Gp24, and Gp25 show
322 surprising similarity to T-even tail fibers in the *Myoviridae* family. Gp25 contains putative
323 collagen-like domains that likely form a triple helical structure, as seen in many other phage tail
324 fibers (26, 27). Gp25 also has a tail tube attachment domain with homology to several other
325 podoviruses (23). Homology analysis via Phyre2 (28) and Hardies et al. (23) revealed that Gp24
326 has regions very similar to P5 of T4 Gp34 and T4 Gp36 (29). P5 Gp34 is one domain of the T4
327 long tail fiber closest to the phage baseplate. T4 Gp35 and Gp36 make up the "knee" of the T4
328 tail long tail fiber (29). None of our ICP2 host-range mutants have Gp24 mutations. Gp23 has
329 both structural (23) and functional homology to T-even adhesins that modulate receptor
330 specificity, such as S16 Gp38 and T4 Gp37 and Gp38 (29-31), suggesting it is the RBP for ICP2.
331 We hypothesize that *gp25* encodes the long portion of the tail fiber attached to the ICP2
332 tail tube. Gp25 host-range mutations possibly allow for more permissive receptor binding by
333 Gp23 by altering tail fiber conformation and therefore adsorption. Furthemore Gp25 and Gp23
334 may interact with independent portions of OmpU or receptors, one of which must be OmpU,
335 altogether. Gp24 makes up the lower long "shin" of a tail fiber and is then distally bound by
336 Gp23, which lies at the tip of each tail fiber. Biochemical and structural studies will be needed to
337 verify this ICP2 tail fiber model. ICP2 Gp14 also has tail fiber homology (23), and we often find
338 missense mutations in this gene, but without selective pressures other than maintaining viability

339 during storage at 4°C (Table S1). Gp14 mutations do not impact Gp23 and Gp25 interactions
340 with OmpU.
341
342 **Application**
343 We have yet to find a secondary receptor for ICP2 and the experiments in this study show
344 that ICP2 is dependent on OmpU as its primary receptor. OmpU is a key *V. cholerae* virulence
345 factor (8, 32), limiting its ability to mutate without fitness costs. Our lab has previously shown
346 that a phage cocktail containing ICP1, ICP2, and ICP3 can be used as prophylaxis in two animal
347 models of *V. cholerae* infection (33). In this therapeutic context, these arms-race limitations help
348 ensure both the specificity and efficacy of ICP2.
349
350 **Materials and Methods**
351 **Strain construction**
352 A mutator strain of *V. cholerae*, designated AC6727 (Table 1), was constructed by
353 moving marked deletions of *mutS* and the K139 prophage into the rough mutant, AC4653, by
354 natural transformation (34). Genomic DNA was purified from strain AC5218 and transformed
355 into AC4653 with selection for spectinomycin resistance (Sp^R). Next, a K139-*att* marked
356 deletion was constructed using splicing-by-overlap-extension (SOE) PCR (2), and tranformed
357 into the *wbeL mutS* double mutant with selection for kanamycin resistance (Km^R). The SOE PCR
358 primers (listed 5' to 3') used were: CCATATAAACAACCTAGCTTCGGC,
359 GCTAATACAACATTGAGCCTTGGTG, GGTTCTCTCGCGTTTTACCCCCACCTTTATC,
360 GGGTAAAACGCGAGAGAACCGGGGCTATTTG, CCAGGCTTTACACTTTATGCTTCC,
361 CCCGTCCTAAAACAATTCATCCAG,

GGAAGCATAAAGTGTAAAGCCTGGGCGTTTTACCCCCACCTTTATC, and CTGGATGAATTGTTTTAGGACGGGGAGAGAACCGGGGCTATTTG. Strains, phages, and plasmids are listed in Table 1.

Bacteriophage isolation and propagation

ICP2_2013_A_Haiti (ICP2) and derivatives were propagated on early exponential growth phase wild-type (WT) *V. cholerae* E7946 (35) growing in Luria Bertani Miller (LB) broth supplemented with streptomycin (100 µg/ ml) at 37°C with aeration. After 3-4 hrs the lysates were centrifuged at 7197 × *g* for 5 min at room temperature (RT) to pellet remaining cells and debris. The supernatants were filtered through 0.22 µm filters and stored as high-titer stocks at 4°C. Stocks were passaged via liquid culture no more than three times to prevent the selection and accumulation of possible mutants. ICP2 stocks were also regularly whole-genome sequenced to authenticate.

Bacteriophage stocks were titered by plaque assay on WT *V. cholerae* within three weeks of being used in experiments. 10 µl of 10-fold serial dilutions of each stock were spotted onto LB 0.3% soft agarose overlays containing approximately 5×10^7 CFU of WT cells and then dribbled across by tilting the plate. Plates were incubated at 37°C overnight (12-18 hrs).

Genetic analysis of phage isolates

Phage gDNA was isolated from high-titer phage stocks by first pretreating with DNase I and RNase A to hydrolyze contaminating host DNA and RNA. Bacteriophage gDNA was then isolated via phenol-chloroform extraction, or using the DNEasy Blood & Tissue kit (Qiagen) according to the kit instructions and including the optional Proteinase K treatment. DNA samples were prepared for sequencing on an Illumina HiSeq2500 using the Nextera XT Kit (Illumina). CLC Genomic Workbench (Version 20, Qiagen) was used to map the resulting reads to the

ICP2_2013_A_Haiti genome (NC_024791.1), and mutations were detected using basic variant detection (Table S2) .

Selection of ICP2 host-range mutants during intestinal infection

All animal experiments were done in accordance with the rules of the Comparative Medicine Services at Tufts University and the Institutional Animal Care and Use Committee. 3-day old infant rabbits were pre-treated with Cimetidine-HCL (Morton Grove Pharmaceuticals) 3 hrs prior to infection (36) and orally inoculated with 5×10^8 CFU of *V. cholerae* in 2.5% sodium bicarbonate (pH 9). A 10:1 mixture of WT to OmpU mutant was used. 5×10^6 PFU of ICP2 was added to the bacteria immediately before inoculation to limit phage adsorption *ex vivo*. Rabbits were euthanized 12 hrs post-inoculation and cecal fluid was collected by dissection and puncture.

Selection of ICP host-range mutants *in vitro*

A mutagenized pool of ICP2 was generated by preparing two independent high-titer stocks on the *V. cholerae* mutator strain AC6727. Selection was performed on each ICP2 stock by adding 10^{10} PFU to a 1 L, mid-exponential phase, 37°C LB broth culture of *V. cholerae* OmpU A182_T193dup. Infection was allowed to proceed overnight. Free phage were purified from the culture supernatant by PEG precipitation. A second, identical selection was performed using the pool of phage purified from each first round selection. Host-range mutants were screened for by plaque assay on the OmpU A182_T193dup mutant. Clear plaque mutants were isolated after each of the second selections, but not from either first selection. Four plaques from each independent selection were plaque-purified on the OmpU A182_T193dup strain. ATdup(1) was isolated from one infection, while ATdup(2) and ATdup(3) were isolated from a second independent infection.

Homologous recombination of ICP2 *gp23* and *gp25* mutations

Mutant alleles of *gp23* and *gp25* from ICP2 host-range mutants were amplified via PCR and cloned into an ampicillin-resistant plasmid, pDL1201 (Figure S3) by blunt-end ligation (Blunt/TA Ligase Master Mix, New England Biolabs). Mutations in *gp23* or *gp25* were cloned into separate plasmids. In order to mitigate toxicity in *Escherichia coli* and *V. cholerae*, amplified fragments excluded the start and stop codons of *gp23* and *gp25*, and the intervening gene, *gp24*, was replaced with a kanamycin resistance gene (*neo)*. *Neo* also separated recombination events occurring within *gp23* and *gp25.* Additionally, the *gp23-neo-gp25* fragment was fused to a LacZα complementing fragment and downstream of a tight arabinose promotor. Recombinant plasmids were first transformed into chemically competent TG1, then moved into *E. coli* SM10(λpir) by electroporation, and finally mated into WT *V. cholerae* or the ΔK139 strain, AC6034. Use of a ΔK139 strain was done to prevent contamination of ICP2 stocks with the K139 temperate phage, which can spontaneously undergo prophage activation.

Plasmid-containing *V. cholerae* strains were grown to early-exponential phase in LB supplemented with ampicillin and/or kanamycin (50 or 100 μg/ml), infected with ICP2 and then incubated at 37°C for 4-5 hours with aeration. During phage multiplication, recombination with the resident plasmid alleles of *gp23* or *gp25* could occur. The high-titer phage stocks from these infections contained both WT and recombinant ICP2.

Host-range and efficiency-of-plaquing (EOP) assays

Stocks of each phage were serially diluted 10-fold and dribbled across (10 μl) or spotted on (5 μl) soft agarose overlays containing either WT *V. cholerae* or an OmpU mutant strain. The plates were incubated at 37°C overnight and PFU were counted. Overlays containing *V. cholerae* Δ*ompU* were included as negative controls representing the absence of plaque formation and to rule out contamination by other phages used in the lab. The EOP of ICP2 host-range mutants was

calculated as the ratio of PFU on an OmpU mutant divided by PFU on WT. EOPs below 1 indicate that an ICP2 mutant cannot infect a mutant OmpU strain as well as it can infect WT. EOPs were averaged from 2-5 replicate infections. Host-range and EOP assays were scanned to better visualize small and/or turbid plaques (EPSON Scan Version 3.25A).

Phage binding assays

Mid-exponential phase cultures of WT *V. cholerae* and OmpU receptor mutant strains were washed and resuspended in LB broth. Each strain was diluted to OD_{600} = 0.1 in 200 µl (~2 × 10^7 CFU) in PCR tubes (USA Scientific, 1402-4700). Three replicates of each strain were heat-killed at 51°C for 12 min and cooled to 37°C for 2 min in a thermocycler and then cooled to RT before adsorption. Examination using a phase-contrast microscope showed that the heating process did not lyse or disrupt the morphology of the cells. Bacteriophage were added to heat-killed cells at a multiplicity of infection (MOI) of 0.1 (~2 × 10^6 PFU). After the addition of phage and mixing, 90 µl were immediately removed and then serially diluted in LB broth to generate a set of samples representing t = 0 hrs of binding. Each dilution series was dribble plated on a soft agarose overlay of WT *V. cholerae*. The remainder of the samples were incubated at RT for 24 hour. After incubation these samples were serially diluted and dribble plated as above. Plates were incubated at 37°C overnight. Binding efficiency was determined as the ratio of PFU at t = 24 hrs to PFU at t = 0 hrs.

Before addition to heat-killed cells, phage stocks with titers below 5 × 10^8 PFU/ml were extracted with 1-octanol to remove LPS (37, 38) and preheated for 1 hr at 37°C to mitigate discrepancies caused by phage disaggregation at RT. This was not necessary for higher titer phage stocks that required 1:10 or 1:100 dilution before addition to heat-killed cells. 1-octanol extraction and preheating did not affect phage predation (Figure S2).

Phage predation killing assays

In a 96-well plate, 100 µl of washed mid-exponential phase *V. cholerae* cells diluted to an OD_{600} = 0.2 were infected with 2×10^7 PFU (MOI = 1) in 100 µl of LB broth supplemented with 100 µg/ml of streptomycin (total volume per well = 200 µl). No-phage controls were included to account for growth differences between the host strains. Infections were done in technical triplicate and incubated at 37°C, with shaking at 205 rpm in a plate reader (BioTeK, Synergy H1). OD_{600} was measured every 5 min over 16 hours. This assay was conducted twice for phage mutants without a genetic replicate (Figure S1).

Acknowledgments

This work was supported by NIH grants GM007310 (ANWL), AI055058 (AC), and AI147658 (AC). AC and MY are associated with and have a financial interest in PhagePro Inc. which is developing a phage cocktail product for prevention of cholera.

References

1. Adhya S, Merril C. 2006. The road to phage therapy. Nature 443:754–755.
2. Letchumanan V, Chan K-G, Pusparajah P, Saokaew S, Duangjai A, Goh B-H, Ab Mutalib N-S, Lee L-H. 2016. Insights into Bacteriophage Application in Controlling Vibrio Species. Front Microbiol 7:66–15.
3. Das B, Verma J, Kumar P, Ghosh A, Ramamurthy T. 2020. Antibiotic resistance in *Vibrio cholerae*: Understanding the ecology of resistance genes and mechanisms. Vaccine 38:A83–A92.
4. Wittebole X, De Roock S, Opal SM. 2014. A historical overview of bacteriophage therapy as an alternative to antibiotics for the treatment of bacterial pathogens. Virulence 5:226–235.
5. Faruque SM, Naser IB, Islam MJ, Faruque ASG, Ghosh AN, Nair GB, Sack DA, Mekalanos JJ. 2005. Seasonal epidemics of cholera inversely correlate with the prevalence of environmental cholera phages. Proc Natl Acad Sci U S A 102:1702–1707.
6. Faruque SM, Islam MJ, Ahmad QS, Faruque ASG, Sack DA, Nair GB, Mekalanos JJ. 2005. Self-limiting nature of seasonal cholera epidemics: Role of host-mediated amplification of phage. Proc Natl Acad Sci U S A 102:6119–6124.
7. Seed KD, Bodi KL, Kropinski AM, Ackermann H-W, Calderwood SB, Qadri F, Camilli A. 2011. Evidence of a dominant lineage of *Vibrio cholerae*-specific lytic bacteriophages shed by cholera patients over a 10-year period in Dhaka, Bangladesh. mBio 2:e00334–10.
8. Seed KD, Yen M, Shapiro BJ, Hilaire IJ, Charles RC, Teng JE, Ivers LC, Boncy J, Harris JB, Camilli A. 2014. Evolutionary consequences of intra-patient phage predation on microbial populations. eLife 3:e03497.

9. Mathur J, Waldor MK. 2004. The *Vibrio cholerae* ToxR-Regulated Porin OmpU Confers Resistance to Antimicrobial Peptides. Infection and Immunity 72:3577–3583.

10. Sakharwade SC, Mukhopadhaya A. 2015. *Vibrio cholerae* porin OmpU induces LPS tolerance by attenuating TLR-mediated signaling. Molecular Immunology 1–13.

11. DiRita VJ, Parsot C, Jander G, Mekalanos JJ. 1991. Regulatory cascade controls virulence in *Vibrio cholerae*. Proc Natl Acad Sci U S A 88:5403–5407.

12. Sperandio V, Giron JA, Silveira WD, Kaper JB. 1995. The OmpU outer membrane protein, a potential adherence factor of *Vibrio cholerae*. Infection and Immunity 63:4433–4438.

13. Wibbenmeyer JA, Provenzano D, Landry CF, Klose KE, Delcour AH. 2002. *Vibrio cholerae* OmpU and OmpT porins are differentially affected by bile. Infection and Immunity 70:121–126.

14. Ante VM, Bina XR, Howard MF, Sayeed S, Taylor DL, Bina JE. 2015. *Vibrio cholerae leuO* Transcription Is Positively Regulated by ToxR and Contributes to Bile Resistance. J Bacteriol 197:3499–3510.

15. Merrell DS, Bailey C, Kaper JB, Camilli A. 2001. The ToxR-Mediated Organic Acid Tolerance Response of *Vibrio cholerae* Requires OmpU. J Bacteriol 183:2746–2754.

16. Li H, Zhang W, Dong C. 2018. Crystal structure of the outer membrane protein OmpU from *Vibrio cholerae* at 2.2 Å resolution. Acta Crystallogr D Struct Biol 74:21–29.

17. Pathania M, Acosta-Gutierrez S, Bhamidimarri SP, Baslé A, Winterhalter M, Ceccarelli M, van den Berg B. 2018. Unusual Constriction Zones in the Major Porins OmpU and OmpT from *Vibrio cholerae*. Structure 26:708–721.e4.

512 18. Zhang Y. 2008. I-TASSER server for protein 3D structure prediction. BMC
513 Bioinformatics 9:40.
514 19. Roy A, Kucukural A, Zhang Y. 2010. I-TASSER: a unified platform for automated
515 protein structure and function prediction. Nature Protocols 5:725–738.
516 20. Yang J, Yan R, Roy A, Xu D, Poisson J, Zhang Y. 2015. The I-TASSER Suite: protein
517 structure and function prediction. Nat Meth 12:7–8.
518 21. McNair K, Aziz RK, Pusch GD, Overbeek R, Dutilh BE, Edwards R. 2017. Phage
519 Genome Annotation Using the RAST Pipeline, pp. 231–238. *In* Bacteriophages. Springer
520 New York, New York, NY.
521 22. Aziz RK, Bartels D, Best AA, DeJongh M, Disz T, Edwards RA, Formsma K, Gerdes S,
522 Glass EM, Kubal M, Meyer F, Olsen GJ, Olson R, Osterman AL, Overbeek RA, McNeil
523 LK, Paarmann D, Paczian T, Parrello B, Pusch GD, Reich C, Stevens R, Vassieva O,
524 Vonstein V, Wilke A, Zagnitko O. 2008. The RAST Server: Rapid Annotations using
525 Subsystems Technology. BMC Genomics 9:75–15.
526 23. Hardies SC, Thomas JA, Black L, Weintraub ST, Hwang CY, Cho BC. 2016.
527 Identification of structural and morphogenesis genes of Pseudoalteromonas phage φRIO-1
528 and placement within the evolutionary history of *Podoviridae.* Virology 489:116–127.
529 24. Dalia AB, McDonough E, Camilli A. 2014. Multiplex genome editing by natural
530 transformation. Proc Natl Acad Sci USA 111:8937.
531 25. De Sordi L, Khanna V, Debarbieux L. 2017. The Gut Microbiota Facilitates Drifts in the
532 Genetic Diversity and Infectivity of Bacterial Viruses. Cell Host and Microbe 1–23.

533 26. Rasmussen M, Jacobsson M, Björck L. 2003. Genome-based identification and analysis of
534 collagen-related structural motifs in bacterial and viral proteins. J Biol Chem 278:32313–
535 32316.
536 27. Engel J, Bächinger HP. 1999. Collagen-like sequences in phages and bacteria.
537 Proceedings of the Indian Academy of Sciences - Chemical Sciences 111:81–86.
538 28. Mezulis S, Yates CM, Wass MN, Sternberg MJE, Kelley LA. 2019. The Phyre2 web
539 portal for protein modeling, prediction and analysis. Nature Protocols 1–14.
540 29. Granell M, Namura M, Alvira S, Kanamaru S, van Raaij M. 2017. Crystal Structure of the
541 Carboxy-Terminal Region of the Bacteriophage T4 Proximal Long Tail Fiber Protein
542 Gp34. Viruses 9:168–12.
543 30. Dunne M, Denyes JM, Arndt H, Loessner MJ, Leiman PG, Klumpp J. 2018. *Salmonella*
544 Phage S16 Tail Fiber Adhesin Features a Rare Polyglycine Rich Domain for Host
545 Recognition. Structure 26:1573–1582.e4.
546 31. Trojet SN, Caumont-Sarcos A, Perrody E, Comeau AM, Krisch HM. 2011. The gp38
547 Adhesins of the T4 Superfamily: A Complex Modular Determinant of the Phage's Host
548 Specificity. Genome Biology and Evolution 3:674–686.
549 32. Lee SH, Hava DL, Waldor MK, Camilli A. 1999. Regulation and temporal expression
550 patterns of *Vibrio cholerae* virulence genes during infection. Cell 99:625–634.
551 33. Yen M, Cairns LS, Camilli A. 2017. A cocktail of three virulent bacteriophages prevents
552 *Vibrio cholerae* infection in animal models. Nat Commun 8:1–7.
553 34. Meibom KL, Blokesch M, Dolganov NA, Wu C-Y, Schoolnik GK. 2005. Chitin induces
554 natural competence in *Vibrio cholerae*. Science 310:1824–1827.

555 35. Levine MM, Black RE, Clements ML, Cisneros L, Saah A, Nalin DR, Gill DM, Craig JP,
556 Young CR, Ristaino P. 1982. The Pathogenicity of Nonenterotoxigenic *Vibrio cholerae*
557 Serogroup 01 Biotype EI Tor Isolated from Sewage Water in Brazil. Journal of Infectious
558 Diseases 145:296–299.
559 36. Kamp HD, Patimalla-Dipali B, Lazinski DW, Wallace-Gadsden F, Camilli A. 2013. Gene
560 Fitness Landscapes of *Vibrio cholerae* at Important Stages of Its Life Cycle. PLoS Pathog
561 9:e1003800.
562 37. Bonilla N, Rojas MI, Netto Flores Cruz G, Hung S-H, Rohwer F, Barr JJ. 2016. Phage on
563 tap–a quick and efficient protocol for the preparation of bacteriophage laboratory stocks.
564 PeerJ 4:e2261–18.
565 38. Szermer-Olearnik B, Boratyński J. 2015. Removal of Endotoxins from Bacteriophage
566 Preparations by Extraction with Organic Solvents. PLoS One 10:e0122672–10.
567 39. Sack RB, Miller CE. 1969. Progressive changes of Vibrio serotypes in germ-free mice
568 infected with *Vibrio cholerae*. J Bacteriol 99:688–695.
569 40. Schild S, Nelson EJ, Camilli A. 2008. Immunization with *Vibrio cholerae* outer
570 membrane vesicles induces protective immunity in mice. Infection and Immunity
571 76:4554–4563.
572 41. Seed KD, Faruque SM, Mekalanos JJ, Calderwood SB, Qadri F, Camilli A. 2012. Phase
573 Variable O Antigen Biosynthetic Genes Control Expression of the Major Protective
574 Antigen and Bacteriophage Receptor in *Vibrio cholerae* O1. PLoS Pathog 8:e1002917.
575

Table 1. Bacterial strains, phages, and plasmids

Strain, plasmid, or phage	Description	Source
WT	*Vibrio cholerae* O1 El Tor Ogawa E7946 (Sm^R)	(39)
AC2846	E7946 *ΔompU*	(40)
AC6034	E7946 ΔK139 prophage	Lab collection
KS714	E7946 Δ*lacZ*::Kan^R, OmpU A182_T193dup	This study
KS769	E7946 Δ*lacZ*::Kan^R, OmpU V324F	This study
KS784	E7946 Δ*lacZ*::Kan^R, OmpU A196_Y198dup	This study
KS785	E7946 Δ*lacZ*::$Spec^R$, OmpU A195T	This study
KS823	E7946 Δ*lacZ*::$Spec^R$, OmpU L319R	(8)
KS824	E7946 Δ*lacZ*::$Spec^R$, OmpU S329L	(8)
KS825	E7946 Δ*lacZ*::$Spec^R$, OmpU N158Y	(8)
KS745	E7946 OmpU G325D	(8)
KS667	E7946 OmpU A196_Y198dup	(8)
KS658	E7946 OmpU A195T	(8)
KS672	E7946 OmpU V324F	(8)
KS822	E7946 OmpU A182_T193dup, *Δlac*Z::$Spec^R$	(8)
AC4653	E7469 Δ*wbeL* (Sm^R)	(41)
AC5218	E7469 Δ*mutS*::*aad9* (Sm^R, Sp^R)	(24)
AC6727	E7946 Δ*wbeL* ΔK139-*att*::*aph* Δ*mutS*::*aad9* (Sm^R, Km^R, Sp^R)	This study
AC5981	*E. coli* TG1	Lab collection
AC89	*E. coli* Sm10λpir	Lab collection
pDL1201	Plasmid backbone for recombination (Amp^R)	Lab collection
pDL1201_gp23-Kan-25	pDL1201_*gp23-neo-gp25*	This study
pDL1201_23_GD(6)	pDL1201_*gp23*(209R)-*neo-gp25*	This study
pDL1201_23_VF(2)	pDL1201_*gp23*(S188A)-*neo-gp25*	This study
pDL1201_25_GD(1)	pDL1201_*gp23-neo-gp25*(D96N, S676A)	This study
pDL1201_25_GD(6)	pDL1201_*gp23-neo-gp25*(K159E and S742P)	This study
pDL1201_25_VF(2)	pDL1201_*gp23-neo-gp25*(S742P)	This study

ICP2	ICP2_2013_A_Haiti (NC_024791.1)	(8)

576

577

578 **Figures**

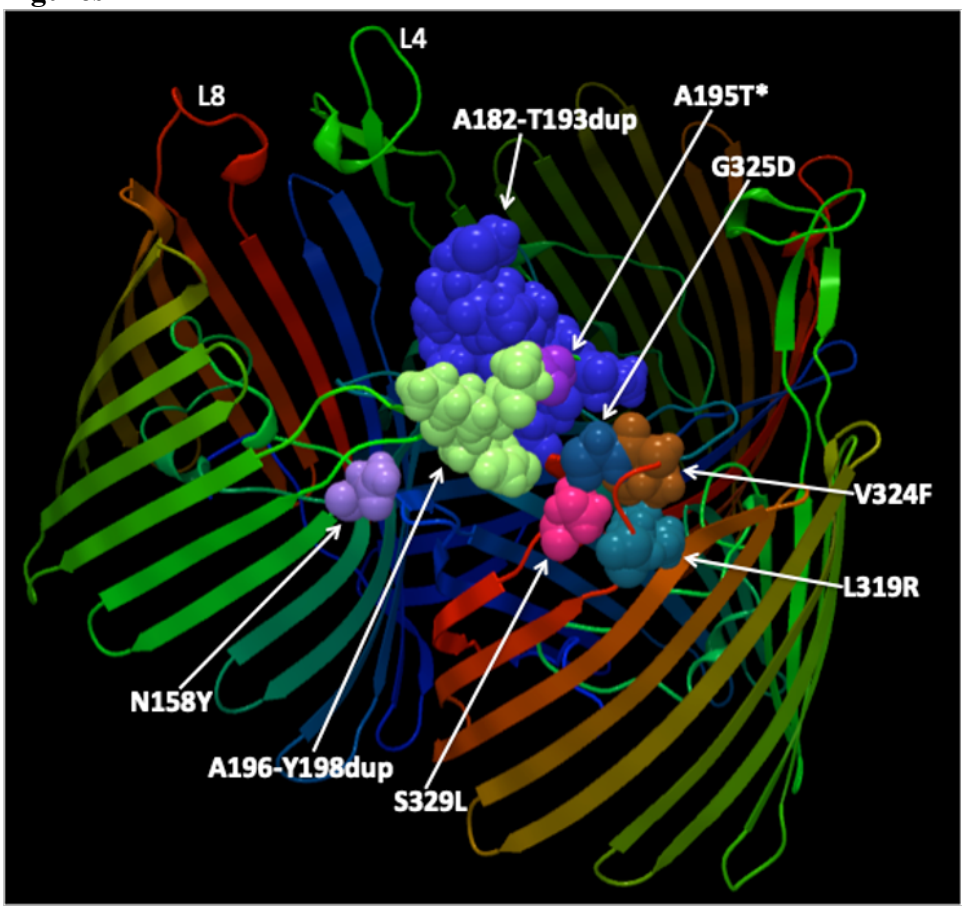

579 **Figure 1. Location of mutated amino acid residues in the OmpU structure that give rise to**
580 **ICP2-resistance.** OmpU mutations previously shown to confer ICP2 resistance (8) map to
581 extracellular loops L4 and L8 on the structure solved by Li et al. (16). The OmpU porin is a
582 homotrimer of three β-barrels. Mutations are highlighted on two adjacent monomers to
583 emphasize their proximity. *Mutation A195T only confers partial resistance to ICP2 (8). This
584 image does not depict how these mutations may affect OmpU structure.
585

586

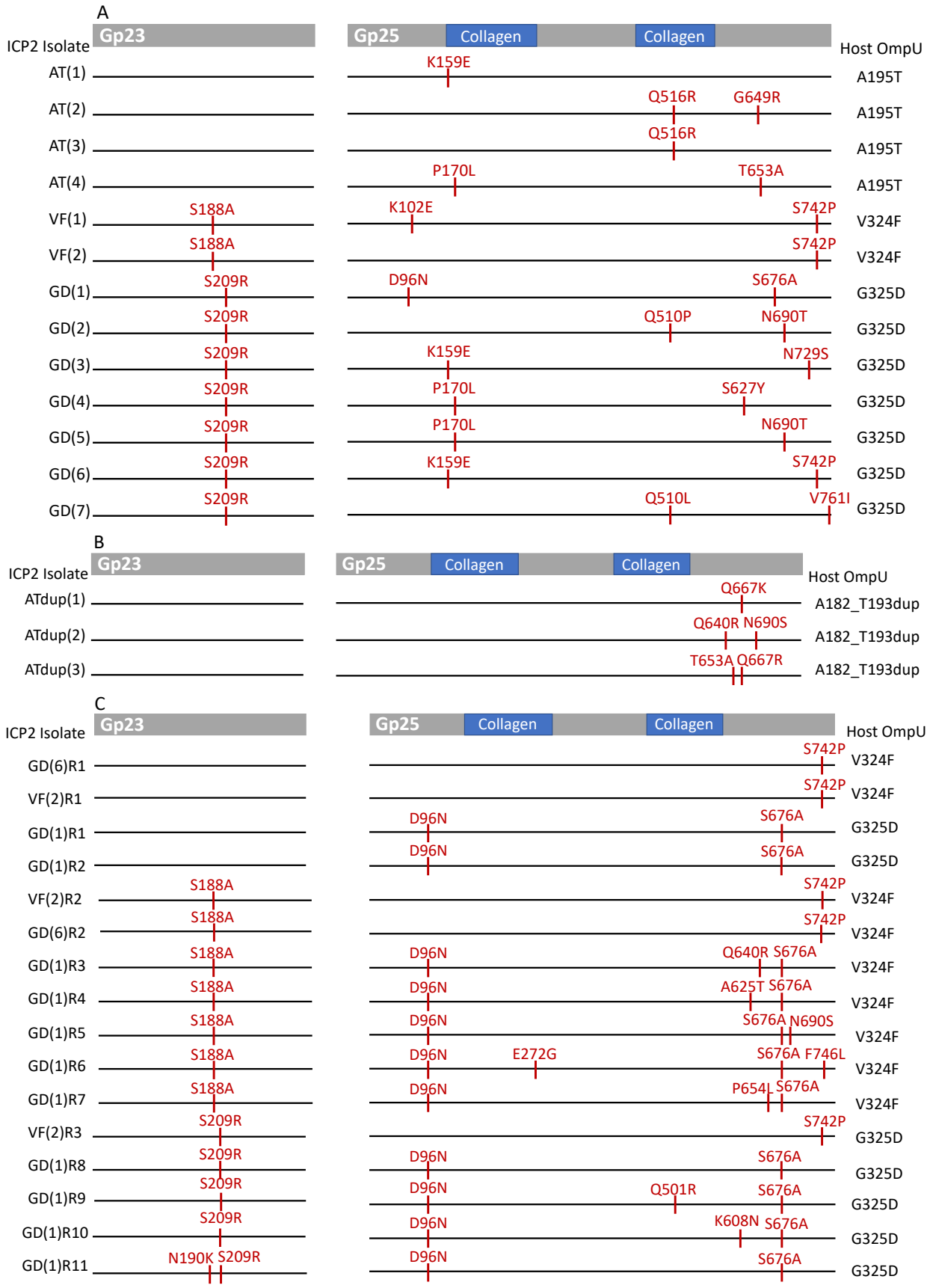

587

Figure 2. ICP2 host-range mutants have missense mutations in *gp23* and *gp25.* Thick grey bars represent the WT amino acid sequence of Gp23 and Gp25, with putative domains indicated where possible. Each pair of thin horizontal lines represents the Gp23 and Gp25 of a single ICP2 mutant (denoted on the left). The mutations present in each isolate are above their corresponding red tick marks. The OmpU allele that each phage mutant was isolated on is indicated on the right. **(A)** ICP2 host-range mutants isolated from the cecal fluid of infant rabbit co-infections had mutations in *gp23* and *gp25*. **(B)** ICP2 host-range mutants selected *in vitro* on OmpU A182_T193dup had mutations in *gp25*. **(C)** Recombinant ICP2 host-range mutants were generated *in vitro* through sequential infections of WT *V. cholerae* strains carrying plasmids with specific *gp23* or *gp25* mutations. Mutants were selected based on their ability to form plaques on either OmpU V324F or OmpU G325D. Gp25 mutations were derived from VF(2), GD(1), and GD(6). Either Gp23 S188A or S209R was then added to these mutants. Several isolates derived from GD(1) acquired one or two novel mutations during the second recombination infection.

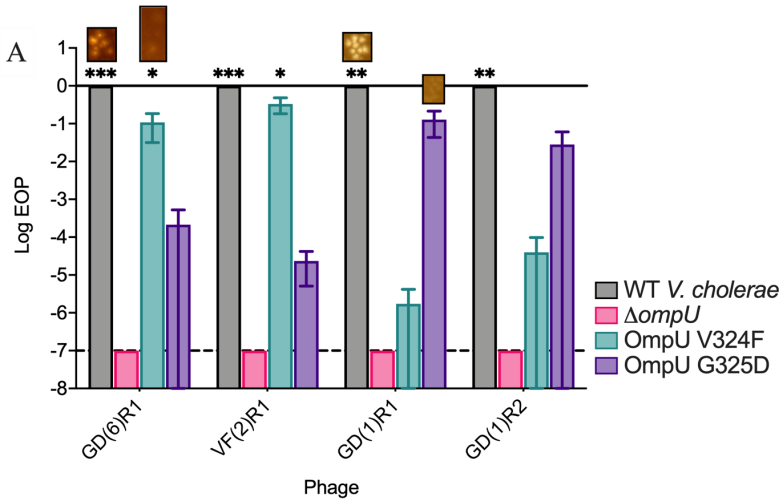

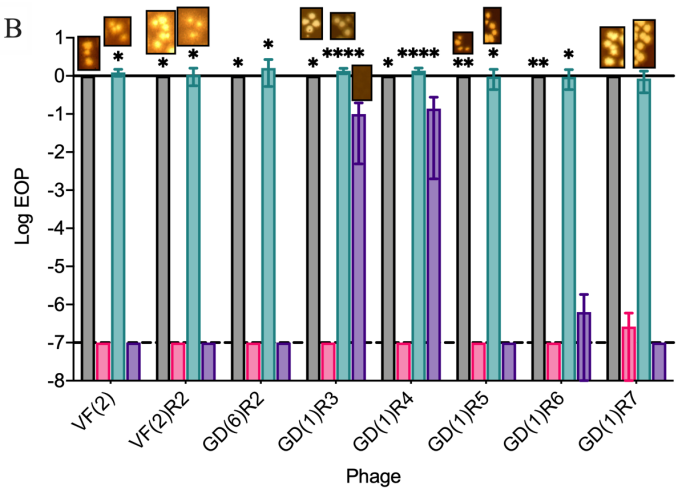

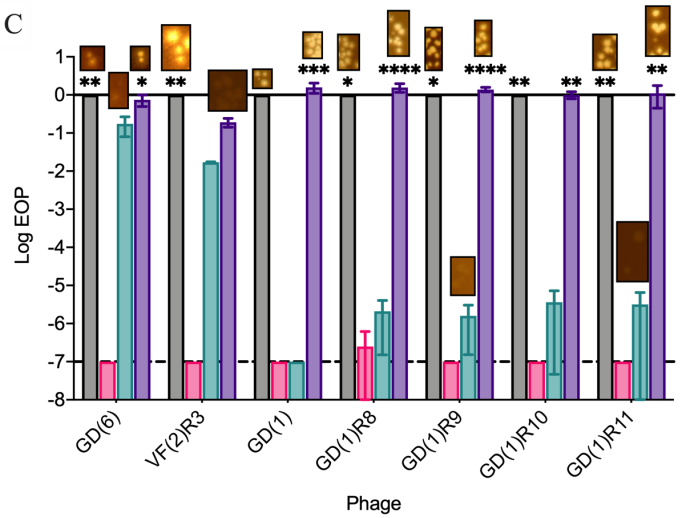

601

Figure 3. Efficiency of Plaquing of ICP2 host-range mutants on OmpU V324F and G325D. EOPs were determined relative to that on WT *V. cholerae*. EOP assays were done in at least quadruplicate with a starting titer of ~10^8 PFU/ml. The dotted line represents the limit of detection and the bars and vertical lines show mean and standard deviation. No data points were included for plaques that were too turbid to count. Examples of plaque morphology are shown above their associated bars. Plaque assays were scanned using Epson scan (V. 3.25A) with adjustments made to contrast and histogram input and output to best visualize turbid plaques. Scanner settings were kept the same for all plates in a single replicate. Statistical significance was determined relative to no plaque formation on Δ*ompU* (Ordinary one-way ANOVA and *post hoc* Dunnett's multiple comparisons test on log-transformed data points). (∗ $P \leq 0.05$, ∗∗ $P \leq 0.01$, ∗∗∗ $P \leq 0.001$, ∗∗∗∗∗ $P \leq 0.0001$) **(A)** Recombinant ICP2 mutants with only one or two Gp25 mutations form turbid plaques on OmpU V324F or OmpU G325D. They also retain the ability to form clear plaques on WT cells. Recombinant isolates GD(6)R1 and VF(2)R1 each have a Gp25 S742P mutation. Recombinant isolates GD(1)R1 and GD(1)R2 contain the two Gp25 mutations found in GD(1). **(B)** ICP2 host-range mutants with secondary Gp23 S188A mutations form clear plaques on OmpU V324F and have EOPs near 1, regardless of their Gp25 mutations. Recombinant isolates GD(1)R3 and GD(1)R4 retain the ability to weakly infect OmpU G325D. **(C)** ICP2 host-range mutants with secondary Gp23 S209R mutations have increased EOPs on OmpU G325D, regardless of their Gp25 mutations.

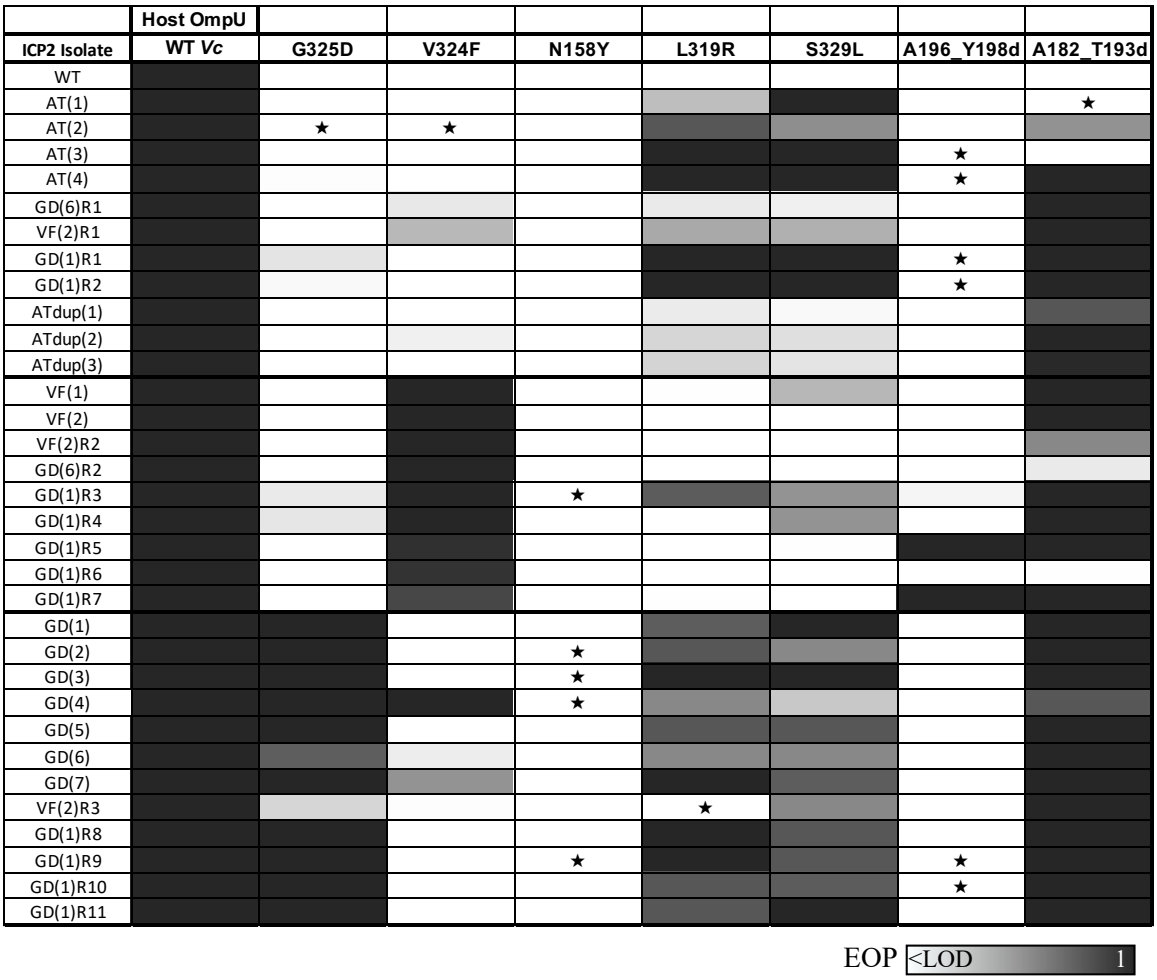

621 **Figure 4. Host-range Efficiency of Plaquing assays on ICP2-resistant OmpU mutants.** Host-
622 range mutants are organized top to bottom rows according to their Gp23 mutations: the top 11,
623 AT(1)-GD(1)R2, have no Gp23 mutation; the middle nine, VF(1)-GD(1)R7, have Gp23 S188A;
624 the lower 11, GD(1)-GD(1)R10, have Gp23 S209R; and the bottom mutant, GD(1)R11, has
625 Gp23 N190K and S209R. Approximate EOPs from below the limit if detection (<LOD) to 1,
626 indicated by the scale-bar, are based on the mean of two to five replicates; averages >1 were set
627 to 1. ICP2 mutants shown in Figure 3 were not retested on OmpU V324F and OmpU G325D;
628 these boxes use the mean EOP values from Figure 3. ★ indicates that lysis at lower dilutions was
629 observed in at least two replicates, without single plaques at higher dilutions.

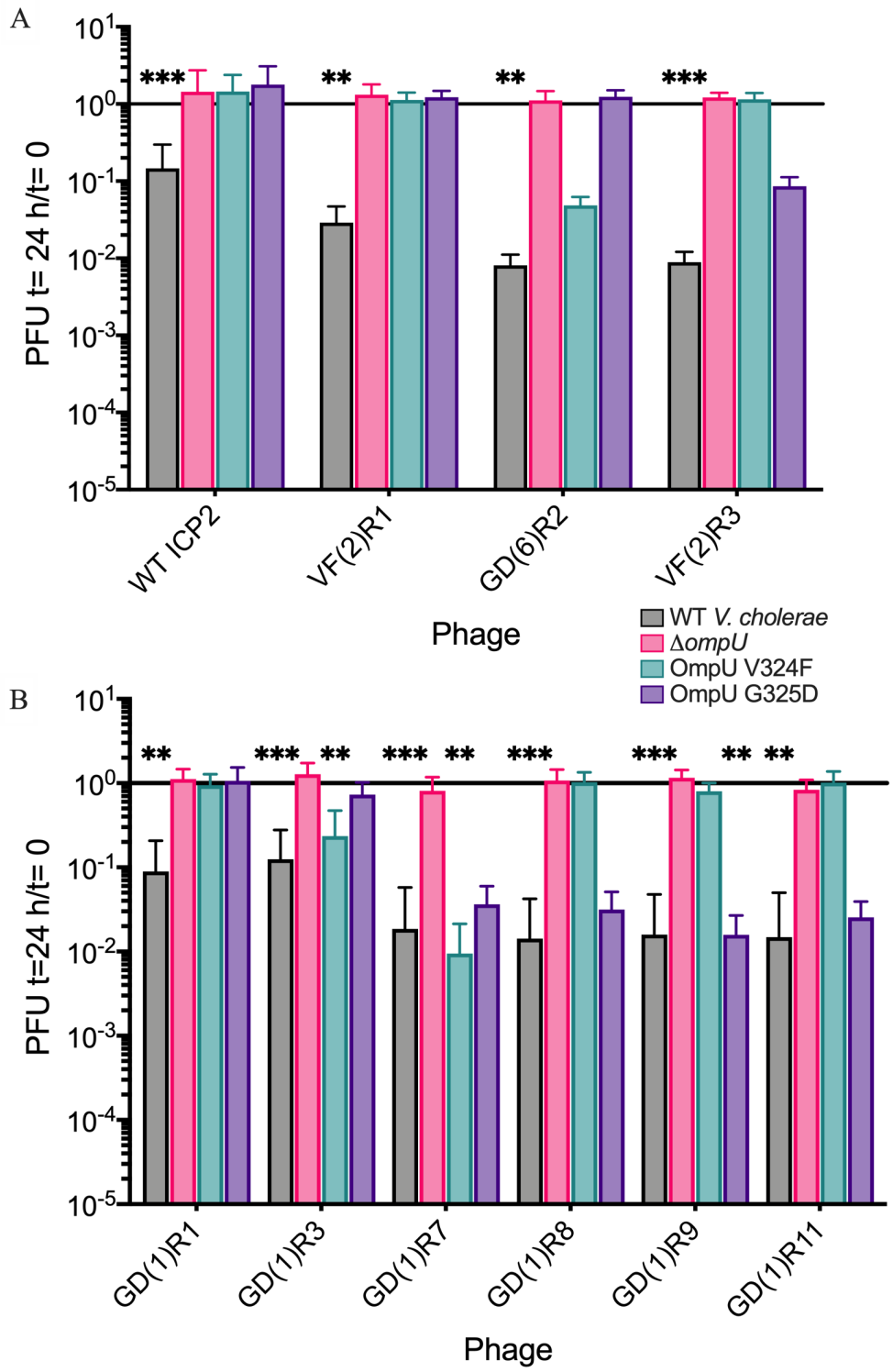

630 **Figure 5. Phage binding to heat-killed OmpU mutant cells.** Phage were added to heat-killed

631 cells at an MOI ~ 0.1 and incubated for 24 hrs at room-temperature. Binding was determined as

632 the ratio between PFU added (t=0) to PFU remaining at t=24 h; a ratio near 1 indicates no

633 detectable binding. Each bar represents the mean and standard deviation of four to 12 biological
634 replicates (WT ICP2 n=12, GD(1)R11 on OmpU G325D n=4, most samples have six to nine
635 biological replicates). Statistical significance was determined relative to no binding to Δ*ompU*
636 (Kruskal-Wallis and *post hoc* Dunn's multiple comparison tests). (∗ $P \leq 0.05$, ∗∗ $P \leq 0.01$, ∗∗∗ P
637 ≤ 0.001, ∗∗∗∗∗ $P \leq 0.0001$). **(A)** WT ICP2 only binds to heat-killed WT *V. cholerae* cells.
638 VF(2)R1 also only binds WT *V. cholerae* despite having a single Gp25 S742P mutation. The
639 addition of Gp23 S188A or S209R is associated with binding to OmpU V324F or G325D,
640 respectively. GD(6)R2 and VF(2)R3 bind OmpU V324F and G325D as expected, but not at
641 statistically significant amounts. **(B)** Similarly, GD(1)R1 has two Gp25 mutations but only binds
642 to WT *V. cholerae*. The addition of Gp23 S188A or S209R results in the ability to bind specific
643 OmpU alleles. Binding to OmpU G325D does not reach statistical significance. GD(1)R7 binds
644 both OmpU alleles despite only forming plaques on OmpU V324F.

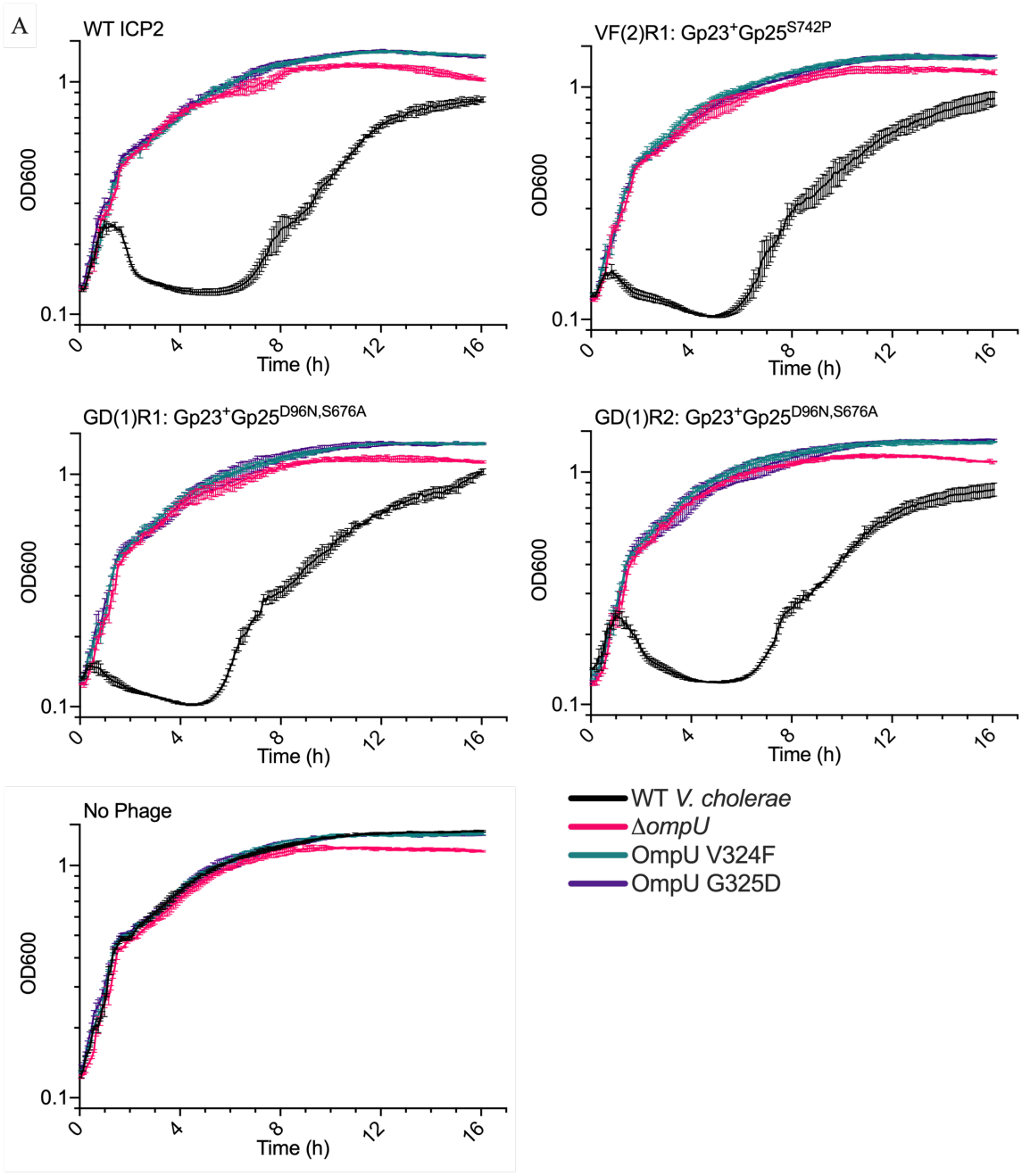

645

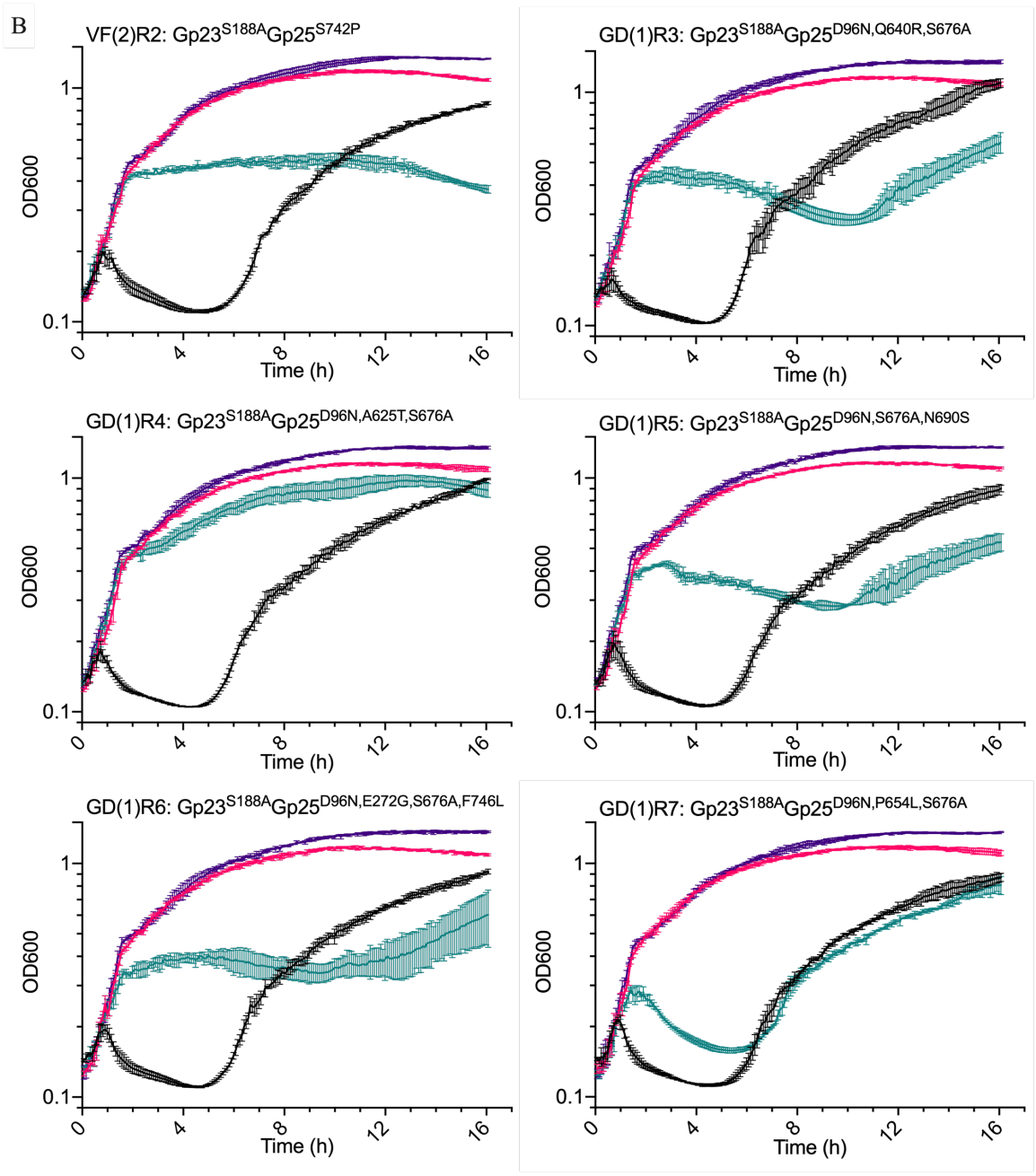

646

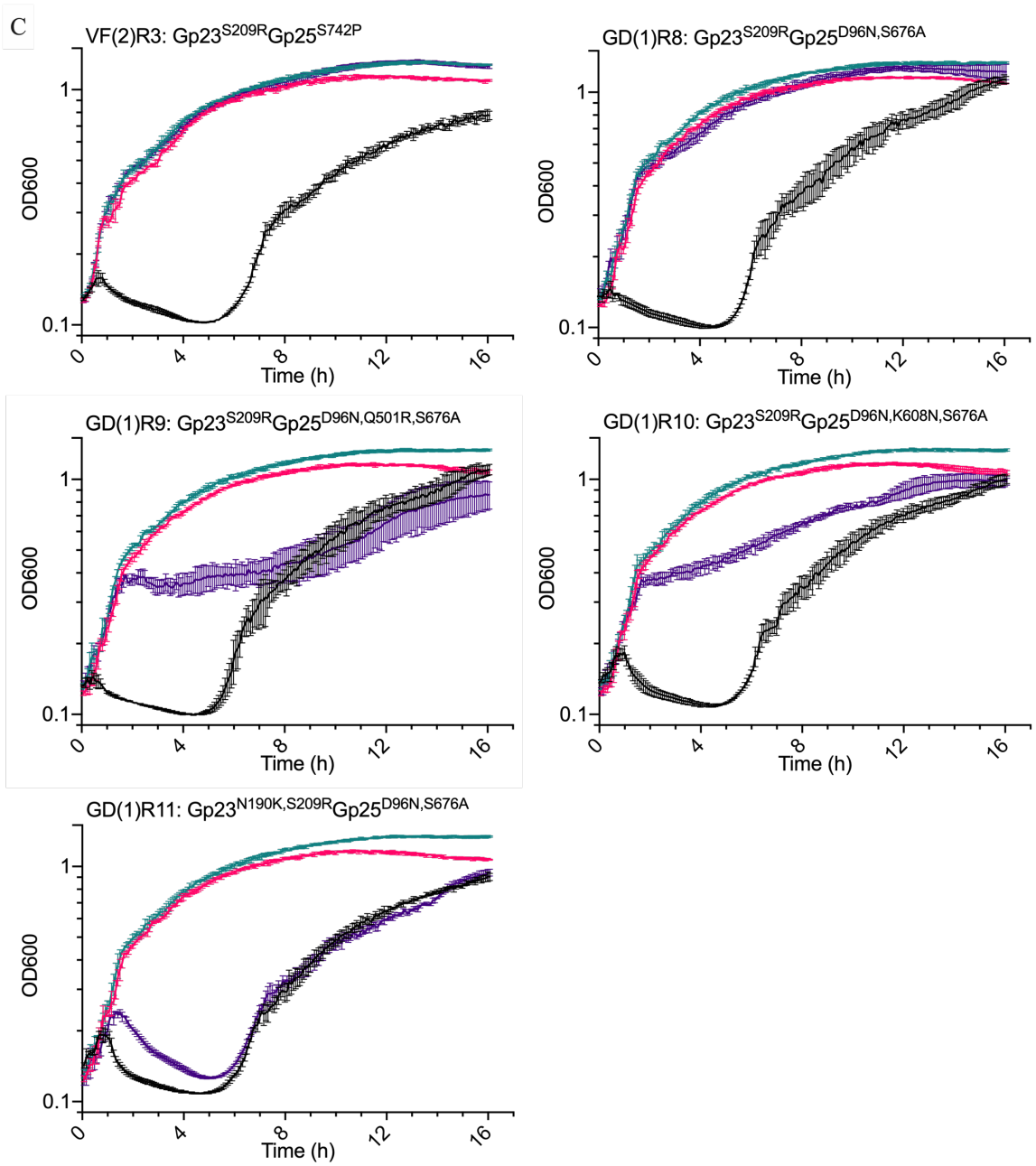

647 **Figure 6. Phage predation killing assays in broth culture.** Killing assays were used to
648 evaluate how different ICP2 mutants prey on actively replicating cultures of WT *V. cholerae*,
649 Δ*ompU*, OmpU V324F, and OmpU G325D. Early- to mid-exponential growth phase cells were
650 infected at an MOI ~1. The optical density at 600 nm was measured every 5 min over 16 hrs at
651 37°C in a BioTek plate reader. Each graph represents the mean of three technical replicates.

652 Error bars represent standard deviation. A no phage control shows that Δ*ompU* has a slight
653 growth defect. **(A)** WT ICP2 can only prey on WT *V. cholerae*. ICP2 host-range mutants with
654 only Gp25 mutations do not effectively kill OmpU V324F or OmpU G325D. **(B)** ICP2 host-
655 range mutants with a secondary Gp23 S188A kill OmpU V324F with varying degrees of
656 efficiency. **(C)** VF(2)R3 does not kill OmpU G325D despite having a secondary Gp23 S209R
657 mutation, corresponding with its lower EOP and turbid plaque morphology on this host. The
658 remaining ICP2 host-range mutants with Gp23 S209R prey on OmpU G325D, but with varying
659 degrees of efficiency.